

# Sticky stuff: Redefining bedform prediction in modern and ancient environments

Robert J. Schindler<sup>1,2</sup>, Daniel R. Parsons<sup>1\*</sup>, Leiping Ye<sup>1</sup>, Julie A. Hope<sup>3</sup>, Jaco H. Baas<sup>4</sup>, Jeff Peakall<sup>5</sup>, Andrew J. Manning<sup>1,2</sup>, Rebecca J. Aspden<sup>3</sup>, Jonathan Malarkey<sup>4</sup>, Steve Simmons<sup>1</sup>, David M. Paterson<sup>3</sup>, Ian D. Lichtman<sup>4,6</sup>, Alan G. Davies<sup>4</sup>, Peter D. Thorne<sup>6</sup>, and Sarah J. Bass<sup>2</sup>

<sup>1</sup>Department of Geography, Environment and Earth Sciences, University of Hull, Hull HU6 7RX, UK

<sup>2</sup>School of Marine Science & Engineering, Plymouth University, Drake Circus, Plymouth PL4 8AA, UK

<sup>3</sup>School of Biology, Scottish Oceans Institute, University of St Andrews, Fife KY16 8LB, UK

<sup>4</sup>School of Ocean Sciences, Bangor University, Menai Bridge, Anglesey LL59 5AB, UK

<sup>5</sup>School of Earth and Environment, University of Leeds, Leeds LS2 9JT, UK

<sup>6</sup>National Oceanography Centre, Joseph Proudman Building, 6 Brownlow Street, Liverpool L3 5DA, UK

## ABSTRACT

**The dimensions and dynamics of subaqueous bedforms are well known for cohesionless sediments. However, the effect of physical cohesion imparted by cohesive clay within mixed sand-mud substrates has not been examined, despite its recognized influence on sediment stability. Here we present a series of controlled laboratory experiments to establish the influence of substrate clay content on subaqueous bedform dynamics within mixtures of sand and clay exposed to unidirectional flow. The results show that bedform dimensions and steepness decrease linearly with clay content, and comparison with existing predictors of bedform dimensions, established within cohesionless sediments, reveals significant over-prediction of bedform size for all but the lowermost clay contents examined. The profound effect substrate clay content has on bedform dimensions has a number of important implications for interpretation in a range of modern and ancient environments, including reduced roughness and bedform heights in estuarine systems and the often cited lack of large dune cross-sets in turbidites. The results therefore offer a step change in our understanding of bedform formation and dynamics in these, and many other, sedimentary environments.**

## INTRODUCTION

Fine-grained mud, made up of silt- and clay-sized particles, is the most abundant material on Earth's surface, and mixed mud-sand environments dominate deltas, tidally dominated rivers, and estuaries (Healy et al., 2002). These systems are among the most sensitive to environmental changes, such as sea-level rise and extreme weather events, which will act to alter a range of sediment transport processes within these environments (FitzGerald et al., 2008). Mud-sand mixtures also dominate a range of deeper marine environments, including shelf seas, the continental slope and rise, and submarine fans (e.g., Talling et al., 2012).

Dune bedforms are important morphological elements of many of these environments and act as primary contributors to sediment flux and boundary roughness, where dune-related roughness is a critical parameter in a range of models used to predict flows and system evolution under changing conditions (e.g., van Rijn, 2007). Dunes are known to scale with flow depth (e.g., van Rijn, 2007), and robust prediction of dune dimensions is therefore crucial for understanding modern systems, including management of engineering infrastructure and waterways. Indeed, the roughness length scales based on predicted dune dimensions are critical parameters in numerical simulations used

to predict flooding and the effects of sea-level change, and to manage engineered waterways (Paarlberg et al., 2010). Moreover, scales of preserved dune sets are a first-order predictor and therefore a key tool for sedimentary environment reconstruction (e.g., Allen, 1982; Paola and Borgman, 1991).

Consequently, dune dynamics have been studied extensively. However, our ability to predict sediment transport rates and dune dimensions in mixed mud-sand environments is severely restricted by a total reliance on cohesionless sediment-based bedform phase diagrams and predictors (e.g., van den Berg and van Gelder, 1993; van Rijn, 2007), despite the broad recognition that physical cohesion imparted by clay within the mud fraction can significantly influence the erosive properties of sediment (e.g., Jacobs et al., 2011) and current ripple dynamics. Here, we assess the influence of bed clay content on dune morphology in a series of controlled flume experiments that represent the conditions in a typical estuarine environment, and compare the experimental results to predictions designed for cohesionless material to elucidate the broader importance of physical cohesion on dune dimensions and dune-derived sedimentary deposits.

## EXPERIMENTAL METHODOLOGY

Experiments were undertaken in a recirculating flume channel 10 m long and 2 m wide (Fig.

DR1 in the GSA Data Repository<sup>1</sup>). A baffle at the inlet removed large-scale turbulence, and a weir at the outlet controlled water surface slope and thus maintained uniform flow conditions over the test section (Fig. DR1). Flow depth was set at  $d = 0.38$  m. Depth-mean flow velocity ( $U$ ) over the initial flat bed set to a zero slope was  $0.80$  m s<sup>-1</sup>, yielding a Froude number  $Fr = U/(gd)^{0.5} = 0.40$  and a Reynolds number  $Re = Udv = 212,000$ , where  $g$  is the acceleration due to gravity and  $\nu$  is the kinematic viscosity. The salinity was 15–17 PSU, approximating estuarine conditions, and temperature was kept as constant as possible, varying between 16 and 19 °C.

Substrates were made using two sediment fractions: a cohesionless fine sand with a median diameter  $D_{50} = 239$   $\mu\text{m}$ , and kaolin clay,  $D_{50} = 3.4$   $\mu\text{m}$ , to represent the cohesive mud fraction (Fig. DR2). Seven substrates were prepared by varying initial bed clay content ( $f_0$ ) from 1.9% (run 1) to 14.1% (run 7) by mass (Table DR1 in the Data Repository). Prior to each experiment, the substrate was homogenized and fully mixed as a wet slurry before being flattened across the whole flume to a thickness of 0.20 m. A flow of  $0.80$  m s<sup>-1</sup> was run for a duration of 10.5 h over each sediment bed. The experiments were designed to fall within the dune bedform field on the bedform phase diagram of van den Berg and van Gelder (1993), used widely to predict bedform type in cohesionless substrates (Fig. 1). This diagram uses a mobility parameter related to grain roughness,  $\theta'$  (van Rijn, 2007), on the ordinate axis and a non-dimensional particle parameter,  $D_*$ , on the abscissa. The experimental phase space used in this study is within the dune regime (Fig. 1), with only a small range of  $D_*$  and  $\theta'$  resulting from the minor changes in particle size distribution between experiments (Fig. DR2).

Bed topography was measured using a 2 MHz ultrasonic ranging sensor mounted on an auto-

<sup>1</sup>GSA Data Repository item 2015142, Figure DR1 (plan view of recirculating flume), Figure DR2 (grain size distributions of sand and kaolin fractions), and Table DR1 (experimental results), is available online at [www.geosociety.org/pubs/ft2015.htm](http://www.geosociety.org/pubs/ft2015.htm), or on request from [editing@geosociety.org](mailto:editing@geosociety.org) or Documents Secretary, GSA, P.O. Box 9140, Boulder, CO 80301, USA.

\*E-mail: [d.parsons@hull.ac.uk](mailto:d.parsons@hull.ac.uk)

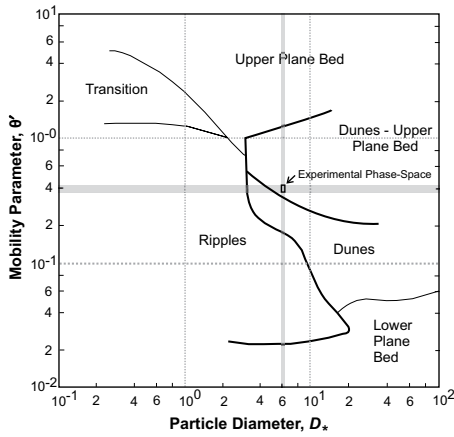


**Figure 1.** Bedform phase diagram (modified after van den Berg and van Gelder, 1993) showing bedform types predicted for experimental flow conditions. Mobility parameter  $\theta' = U^2/(s-1)C'^2D_{50}$  (where  $U$  is depth-mean flow velocity,  $D_{50}$  is median grain diameter,  $s$  is relative density of sediment, and  $C'$  is Chézy coefficient related to grain roughness), and non-dimensional particle diameter  $D_* = D_{50}[(s-1)g/v^2]^{0.33}$  (where  $g$  is acceleration due to gravity and  $v$  is kinematic viscosity) vary with grain-size distribution of each substrate. Maximum suspended sediment concentration observed across all experiments was  $\sim 2.2$  g/L.  $\theta' = 0.38$  for sand fraction only, and increases to 0.41 as initial clay fraction is increased to 14.1%.  $D_* = 6.4$  for sand fraction only, with  $D_* = 5.95$  for highest initial clay fraction. Influence of effective viscosity variations between experiments, caused by temperature change ( $<4$  °C) and suspended load of kaolinite ( $<1\%$  by volume), are also small (Southard and Boguchwal, 1990; De Wit, 1992). Consequently, despite these variations, dunes are predicted in all cases.

mated traverse, oriented along the center of the flume over a 3.5-m-long test section (Fig. DR1), enabling measurement of dune dimensions. Dunes were distinguished from superimposed ripples by their longer length and laterally continuous crests that stretched across the width of the channel (Reesink and Bridge, 2007). After 10.5 h, the individual heights and lengths of each dune were determined and mean values ( $H$ ,  $L$ ) calculated for each experiment. Flow velocity was monitored at 25 Hz during each experiment run using four vertically stacked, 10 MHz acoustic Doppler velocimeters close to the flume centerline (Fig. DR1).

### EXPERIMENTAL RESULTS

The experimental results reveal a dramatic influence of initial bed clay content on mean bedform height, length, and steepness ( $H/L$ ) (Figs. 2 and 3). The final bed topographies for runs 1–7 (Fig. 2) show a clear transition from fully three-dimensional dune-scale bedforms for  $f_0 = 1.9\%$  (run 1), through lower-angle, flatter dunes for  $4.7\% < f_0 < 9.8\%$  (runs 2–4) and very low-angle dunes partly masked by current ripples for  $f_0 = 11.9\%$  (run 5), to surfaces that approach a flat bed for  $12.7\% < f_0 < 14.1\%$  (runs 6–7). Figure 3 shows a statistically significant, negative linear correlation between mean bedform height and initial bed clay content across the experiments (Fig. 3A), with  $H = 88$  mm for  $f_0 = 1.9\%$  (run 1) and  $H = 8$  mm for  $f_0 = 14.1\%$  (run 7) (Table DR1), as well as negative linear correlation between mean bedform length and initial bed clay content (Fig. 3B), with  $L = 1634$  mm for  $f_0 = 1.9\%$  and  $L = 690$  mm for  $f_0$

$= 14.1\%$  (Table DR1). Bedform steepness also decreases as  $f_0$  increases (Figs. 3C and 3D; Table DR1). Hence, the bedforms in clay-rich sand have lower amplitudes, lower wavelengths, and flatter geometries than in clay-poor sand. Particularly remarkable is the order-of-magnitude reduction in bedform height. Figure 3A includes predictions of equilibrium bedform height, using the classical method of van Rijn (1984). Based on the median grain sizes in the experimental runs, these predictions range from  $H = 76.5$  mm (1.9% clay) to  $H = 73.9$  mm (14.1% clay). These predicted heights are considerably larger than the majority of the observed heights in the mixed sand-clay substrate. Only the observed dune height in run 1, at low clay content ( $f_0 = 1.9\%$ ), is close to the predicted values. The substrates with higher clay content systematically depart from the predicted bedform height by up to 900% ( $f_0 = 14.1\%$ ). Figure 3B shows a predicted equilibrium bedform length of 2770 mm (van Rijn, 1984). This prediction is well in excess of the measured lengths, overestimating these values by 42% for run 1 and by 400% for run 7. The influence of substrate clay content extends to bedform steepness, which is inversely related to clay content and below predictions for all but the run with the lowest bed clay content ( $f_0 = 1.9\%$ ) (Ashley, 1990).

### DISCUSSION

The experimental data show that bedforms in substrates composed of sand-clay mixtures are modified substantially in shape and size by increasing levels of cohesive clay. Increasing levels of clay result in progressively smaller

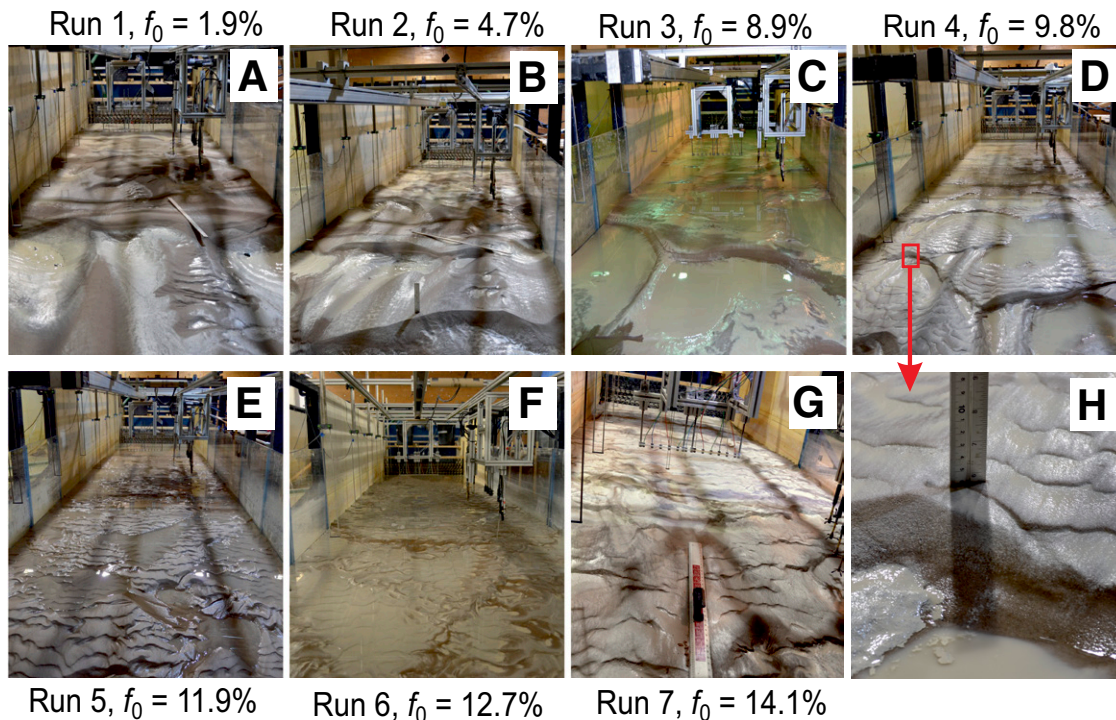
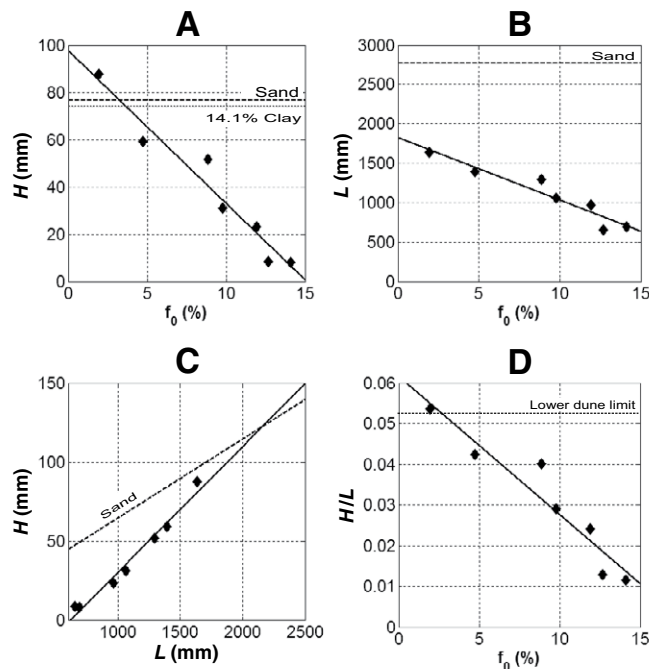


**Figure 2.** Final bed morphology of experiment runs 1–7. A–G: Bed morphologies viewed from distal end over measurement domain, showing decreasing bedform size as clay content ( $f_0$ ) increases, resulting in markedly different bedform types. Runs 1–3, full dune forms; runs 4–5, dunes with superimposed ripples; runs 6–7, ripples with decreasing crestline sinuosity. H: Close-up of dune crest with superimposed ripples for run 4, with ruler for scale.

**Figure 3. A: Relationship between dune height,  $H$ , and initial clay content,  $f_0$  ( $R^2 = 0.95$ ). Dotted lines are the predicted equilibrium height for both pure sand and mixed sand-clay with highest initial clay content, assuming no cohesion (van Rijn, 1984). B: Relationship between dune wavelength,  $L$ , and initial clay content ( $R^2 = 0.92$ ). Dotted line is the predicted equilibrium wavelength (van Rijn, 1984). C: Relationship between  $H$  and  $L$  ( $R^2 = 0.97$ ). Also shown is predicted relationship for pure sand according to Ashley (1990). D: Relationship between bedform steepness,  $H/L$ , and initial clay content ( $R^2 = 0.91$ ). Also shown is lower limit of dune steepness according to Ashley (1990).**



bedforms, with reduced heights, lengths, and steepness. The bedforms transition from very low-angle forms toward a flat bed at the highest clay levels ( $f_0 > \sim 12\%$ ). The deviation from the accepted predictions of bedform size within mixed sediment substrates has significant implications for paleoenvironmental and other geological interpretations in a range of environments. Bedforms in general are the primary predictor used in paleoenvironmental reconstructions of sedimentary successions formed by waves and currents, and dunes in particular are used to reconstruct paleoflow depth for open-channel flows (e.g., Leclair and Bridge, 2001). The suppression of bedform size with increased substrate clay detailed herein could therefore result in significant misinterpretations of paleoenvironmental conditions and may also result in the underestimation of paleodepths by up to an order or magnitude. Cross-stratification may also be hard to recognize in the deposits of the flatter bedforms, in which case their utility as predictors for paleodepth may be entirely lost. In addition, there is potential for misinterpretation of the nature of bedforms because dune height decreases (dunes become washed out) toward the upper velocity limit of dune stability prior to formation of an upper-stage plane bed (Rubin and Carter, 2006). Similar adjustments are produced by the higher clay contents such that cross-sets formed where substrate clay content is high (here  $f_0 > 12\%$ ) may be misinterpreted as bedforms close to the upper-stage plane bed.

These experiments may also provide an explanation for the “dune paradox” observed in deep-marine turbidite beds, where dunes do

not typically form despite flows decelerating from upper-stage plane beds, through the dune bedform phase space, to ripples (Arnott, 2012). Previous explanations have focused on (1) flow duration, (2) insufficiently coarse grain size in deposits, (3) high sediment fall-out rates, and (4) cohesive flow-driven changes in turbulence. Arnott (2012) argued that these mechanisms were all improbable, instead proposing a model where amplification of initial perturbations was restricted by very high bedload concentrations commensurate with that of the bedload layer. Such high basal concentrations would appear unlikely however for all but the most rapidly collapsing turbidity currents. Here we propose that it is the composition of the bed that could be key to this dune paradox. There has been increasing recognition of the prevalence of mud-rich sand beds (up to 40%–50% mud) within turbidite sequences, and that the mud composition of even clean turbiditic sands is  $\sim 5\%$ – $10\%$  or higher (Talling et al., 2013; Stevenson et al., 2014). The presence of such mud within turbiditic sands will either restrict dune development entirely (mud-rich sands) or favor the formation of small, low-relief bedforms (clean sands) that may be characterized by small-scale wavy bedding as commonly observed in turbidite sequences (Prave and Duke, 1990). The postulated model may explain, for the first time, the widespread absence of dunes under the range of flow types now recognized in sediment gravity flows (Talling et al., 2012), in contrast to the specific requirement of high basal concentrations near the packing limit as proposed in the Arnott (2012) model.

The experimental results also have implications for the morphodynamics of modern sedimentary environments, with scour depths around infrastructure presently being over-predicted in mixed-cohesive environments. Knowledge of dune dimensions is also crucial from modeling perspectives (Sutherland et al., 2004) as it is a key parameter in a range of numerical flow and sediment transport models. The velocity of a turbulent flow varies with the inverse logarithm of the roughness height, thus models are highly dependent on the accurate representation of the form roughness contribution to effective roughness height (e.g., Morvan et al., 2008). Spatial and temporal variations in sediment composition, and hence bedform size and morphology, will lead to inaccuracies in numerical model output where roughness heights, based on cohesionless sands, are often prescribed for the model domain (e.g., Sutherland et al., 2004). Schemes with spatially varying roughness heights are typically derived from known grain sizes within the domain (e.g., Soulsby, 1997). However, these approaches do not currently account for cohesive effects on dune dimensions and resultant reductions in form roughness.

Finally, these experiments have demonstrated the profound effect of a weakly bonding clay (kaolinite) on bedform size. The presence of a clay mineral with superior bonding kinetics, such as a dioctahedral smectite (e.g., montmorillonite), may suppress dune evolution at an even lower clay percentage. Moreover, physical cohesion imparted by clay is not the only source of relative substrate stability compared with pure, cohesionless sediments. Additional cohesive strength can result from further physical, biological, and geochemical properties including: initial water content and compaction (Molinas et al., 1999), mineralogy (e.g., Alizedah, 1974), and biological stabilization (Paterson et al., 1990), particularly through the secretion of large quantities of extracellular polymeric substances ubiquitous to estuarine muds (Hoagland et al., 1993). It is imperative that physical cohesion imparted by substrate clay content, and other similar cohesive effects, are considered and included within the next-generation bedform predictors.

## CONCLUSIONS

This paper highlights the hitherto rarely acknowledged importance of physical cohesion on bedform morphology within a range of environments. We show that physical cohesion imparted by clay reduces bedform height, length, and steepness, ultimately yielding different bedforms for different substrate clay content percentages. This has a range of important consequences and implications. Our interpretations of ancient sedimentary sequences that are based on well-used relationships between cross-set characteristics, dune morphology, and formative flow

conditions in cohesionless sediments need to be revisited. Similarly, understanding of modern dune dynamics needs to account for the modification of process and morphology of bedforms in mixed sand-clay sediment for a host of modeling and environmental management applications.

In conclusion, current predictive or interpretative methods designed for use on cohesionless substrates but employed for substrates containing a clay fraction will be misleading. A consideration of physical cohesion needs to be incorporated into such predictions as, at present, these effects are poorly constrained. Figure 4 presents a modified version of the phase-space diagram shown in Figure 1 that includes a new  $z$ -axis incorporating bed clay content. Although this study only examined a single location in the phase space, it shows how knowledge of initial clay content and cohesion is imperative for accurate determination of bedform type. It is reasonable to expect clay cohesion to exert an influence on bed morphology at all combinations of  $\theta'$  and  $D_*$ , and such effects need to be quantified and included in future generations of bedform prediction models.

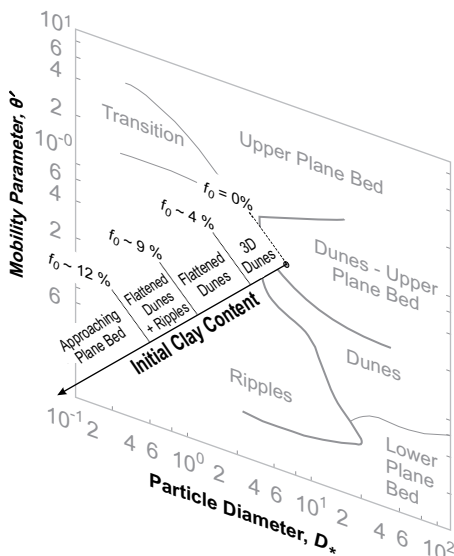


**Figure 4. Conceptual modification of phase-space diagram that includes third axis to incorporate cohesion. The  $z$ -axis shows approximate boundaries of initial clay content ( $f_0$ ) that distinguish between bedform types for the experimental conditions (modified after van den Berg and van Gelder, 1993).**

#### ACKNOWLEDGMENTS

This work was funded by the UK Natural Environment Research Council (NERC) under the COH-BED project (NE/1027223/1). Paterson was funded by the Marine Alliance for Science and Technology

for Scotland (MASTS). Brendan Murphy, Karen Scott, Mark Anderson, Arjan Reesink, Claire Keevil, Chris Unworth, Robert Thomas, Xuxu Wu, and Stuart McLelland are thanked for their help in running the laboratory experiments. We thank G. Postma, L. Hajek, and J. Southard for thoughtful reviews. The experimental data used here are available from the corresponding author on request. Finally, funding for making the article Open Access was provided by the Universities of Hull and Plymouth.

#### REFERENCES CITED

- Alizedah, A., 1974, Amount and type of clay and pore fluid influence on the critical shear stress and swelling of cohesive soils [Ph.D. thesis]: Davis, California, University of California–Davis, 216 p.
- Allen, J.R.L., 1982, Sedimentary Structures: Their Character and Physical Basis: Amsterdam, Elsevier, v. 1, 645 p.
- Arnott, R.W.C., 2012, Turbidites, and the case of the missing dunes: *Journal of Sedimentary Research*, v. 82, p. 379–384, doi:10.2110/jsr.2012.29.
- Ashley, G.M., 1990, Classification of large-scale subaqueous bedforms: A new look at an old problem: *Journal of Sedimentary Petrology*, v. 60, p. 160–172, doi:10.2110/jsr.60.160.
- De Wit, P.J., 1992, Rheological measurements on artificial muds: Delft, Netherlands, Department of Civil Engineering, Delft University of Technology, Report Number 9-92, 29 p.
- FitzGerald, D.M., Fenster, M.S., Argow, B.A., and Buynevich, I.V., 2008, Coastal impacts due to sea-level rise: *Annual Review of Earth and Planetary Sciences*, v. 36, p. 601–647, doi:10.1146/annurev.earth.35.031306.140139.
- Healy, T., Wang, Y., and Healy, J.A., 2002, Muddy Coasts of the World: Processes, Deposits and Function: Amsterdam, Elsevier, 556 p.
- Hoagland, K.D., Rosowski, J.R., Gretz, M.R., and Roemer, S.C., 1993, Diatom extracellular polymeric substances: Function, fine structure, chemistry, and physiology: *Journal of Phycology*, v. 29, p. 537–566, doi:10.1111/j.0022-3646.1993.00537.x.
- Jacobs, W., Le Hir, P., Van Kesteren, W., and Cann, P., 2011, Erosion threshold of sand-mud mixtures: *Continental Shelf Research*, v. 31, p. S14–S25, doi:10.1016/j.csr.2010.05.012.
- Leclair, S.F., and Bridge, J.S., 2001, Quantitative interpretation of sedimentary structures formed by river dunes: *Journal of Sedimentary Research*, v. 71, p. 713–716, doi:10.1306/2DC40962-0E47-11D7-8643000102C1865D.
- Molinas, A., Jones, S. and Hosny, M., 1999, Effects of cohesive material properties on local scour around piers: *Transportation Research Record*, v. 1690, p. 164–174, doi:10.3141/1690-19.
- Morvan, H., Knight, D., Wright, N., Tang, X., and Crossley, A., 2008, The concept of roughness in fluvial hydraulics and its formulation in 1D, 2D and 3D numerical simulation models: *Journal of Hydraulic Research*, v. 46, p. 191–208, doi:10.1080/00221686.2008.9521855.
- Paarlberg, A.J., Dohmen-Janssen, C.M., Hulscher, S.J.M., Termes, P., and Schielen, R., 2010, Modelling the effect of time-dependent river dune evolution on bed roughness and stage: *Earth Surface Processes and Landforms*, v. 35, p. 1854–1866, doi:10.1002/esp.2074.
- Paola, C., and Borgman, L., 1991, Reconstructing random topography from preserved stratification: *Sedimentology*, v. 38, p. 553–565, doi:10.1111/j.1365-3091.1991.tb01008.x.
- Paterson, D.M., Crawford, R.M., and Little, C., 1990, Subaerial exposure and changes in the stability of intertidal estuarine sediments: *Estuarine, Coastal and Shelf Science*, v. 30, p. 541–556, doi:10.1016/0272-7714(90)90091-5.
- Prave, A.R., and Duke, W.L., 1990, Small-scale hummocky cross-stratification in turbidites: A form of antidune stratification?: *Sedimentology*, v. 37, p. 531–539, doi:10.1111/j.1365-3091.1990.tb00152.x.
- Reesink, A.J.H., and Bridge, J.S., 2007, Influence of superimposed bedforms and flow unsteadiness on formation of cross strata in dunes and unit bars: *Sedimentary Geology*, v. 202, p. 281–296, doi:10.1016/j.sedgeo.2007.02.005.
- Rubin, D.M., and Carter, C.L., 2006, Bedforms and cross-bedding in animation, in *Cross-Bedding, Bedforms, and Paleocurrents: SEPM (Society for Sedimentary Geology) Atlas 2*, digital media.
- Soulsby, R.L., 1997, *Dynamics of Marine Sands*: London, Thomas Telford, 249 p.
- Southard, J.B., and Boguchwal, L.A., 1990, Bed configurations in steady unidirectional water flows: Part 3. Effects of temperature and gravity: *Journal of Sedimentary Petrology*, v. 60, p. 680–686, doi:10.2110/jsr.60.680.
- Stevenson, C.J., Talling, P.J., Masson, D.G., Sumner, E.J., Frenz, M., and Wynn, R.B., 2014, The spatial and temporal distribution of grain-size breaks in turbidites: *Sedimentology*, v. 61, p. 1120–1156, doi:10.1111/sed.12091.
- Sutherland, J., Walstra, D.J.R., Chesher, T.J., van Rijn, L.C., and Southgate, H.N., 2004, Evaluation of coastal area modelling systems at an estuary mouth: *Coastal Engineering*, v. 51, p. 119–142, doi:10.1016/j.coastaleng.2003.12.003.
- Talling, P.J., Masson, D.G., Sumner, E.J., and Malgesini, G., 2012, Subaqueous sediment density flows: Depositional processes and deposit types: *Sedimentology*, v. 59, p. 1937–2003, doi:10.1111/j.1365-3091.2012.01353.x.
- Talling, P.J., Malgesini, G., and Felletti, F., 2013, Can liquefied debris flows deposit clean sand over large areas of sea floor? Field evidence from the Marnoso-arenacea Formation, Italian Apennines: *Sedimentology*, v. 60, p. 720–762, doi:10.1111/j.1365-3091.2012.01358.x.
- van den Berg, J.H., and van Gelder, A., 1993, A new bedform stability diagram, with emphasis on the transition of ripples to plane bed in flows over fine sand and silt, in *Marzo, M., and Puigdefàbregas, C., eds., Alluvial Sedimentation: International Association of Sedimentologists Special Publication 17*, p. 11–21.
- van Rijn, L.C., 1984, Sediment transport, Part III: Bed forms and alluvial roughness: *Journal of Hydraulic Engineering*, v. 110, p. 1733–1754, doi:10.1061/(ASCE)0733-9429(1984)110:12(1733).
- van Rijn, L.C., 2007, *Principles of Sediment Transport in Rivers, Estuaries and Coastal Seas, Parts 1 and 2*: Amsterdam, Aqua Publications, 1200 p.

Manuscript received 10 September 2014

Revised manuscript received 3 February 2015

Manuscript accepted 11 February 2015

Printed in USA